Kaohsiung Journal of Medical Sciences (2013) 29, 229–233

Available online at www.sciencedirect.com

SciVerse ScienceDirect

journal homepage: http://www.kjms-online.com

CASE REPORT

Bone metastasis versus bone marrow metastasis? Integration of diagnosis by ^{18}F-fluorodeoxyglucose positron emission/computed tomography in advanced malignancy with super bone scan: Two case reports and literature review

Chia-Yang Lin [a], Yu-Wen Chen [a,e,*], Chin-Chuan Chang [a], Wen-Chi Yang [b], Chih-Jen Huang [c,d,e], Ming-Feng Hou [d,e]

[a] *Department of Nuclear Medicine, Kaohsiung Medical University Hospital, Kaohsiung, Taiwan*
[b] *Division of Hematology, Department of Internal Medicine, Kaohsiung Medical University Hospital, Kaohsiung, Taiwan*
[c] *Department of Radiation Oncology, Kaohsiung Medical University Hospital, Kaohsiung, Taiwan*
[d] *Cancer Center, Kaohsiung Medical University Hospital, Kaohsiung, Taiwan*
[e] *Department of Medicine, College of Medicine, Kaohsiung Medical University, Kaohsiung, Taiwan*

Received 5 April 2012; accepted 29 June 2012
Available online 29 November 2012

KEYWORDS
Breast cancer;
Computed tomography;
^{18}F-fluorodeoxyglucose positron emission tomography;
Gastric cancer;
Super bone scan

Abstract Super scan pattern on technetium-99m methyldiphosphonate (Tc-99m MDP) bone scintigraphy is a special condition of extremely high bone uptake relative to soft tissue with absent or faint renal radioactivity visualization, which is usually seen in diffuse bone metastases or discrete endocrine entities. Here, two cases with super bone scan are presented. One was a young man diagnosed with gastric cancer. The other was a middle-aged woman with a history of breast cancer with recent recurrence. Both cases had 18-fluorodeoxyglucose positron emission tomography/computed tomography (^{18}F-FDG PET/CT) diagnosis simultaneously. Based on imaging of ^{18}F-FDG PET/CT, diffusely incremental ^{18}F-FDG avidity in spine/pelvis on PET and subtle erosion of cortical bone on CT were seen. The cytological results of bone marrow biopsy showed evidence of malignant metastasis. However, there were several focal discrepant findings between the ^{18}F-FDG PET/CT and Tc-99m MDP bone scan. According to integration of both imaging findings and the result of bone marrow biopsy, we believe that the

* Corresponding author. Department of Nuclear Medicine, Kaohsiung Medical University Hospital, No. 100 Tzyou 1st Road, San-Ming District, Kaohsiung, Taiwan.
E-mail address: 800175@ms.kmuh.org.tw (Y.-W. Chen).

http://dx.doi.org/10.1016/j.kjms.2012.08.038

disseminated malignant spread in bone marrow is a primitive alternation in the super bone scan and that it is also as a result of neoplasm-related endocrine factors.

Introduction

Whole body technetium-99m methyldiphosphonate (Tc-99m MDP) bone scan is one of the most commonly performed radionuclide examinations. The normal skeletal-to-renal ratio of absorption of radioisotope is 40—60% [1,2]. A super scan is defined as a bone scan that demonstrates markedly increased skeletal radioisotope uptake relative to soft tissue, and it is usually associated with absent or faint genitourinary tract radioactivity [3]. Similar to the super scan of bone scintigraphy, fluorine-18-fluorodeoxyglucose positron emission tomography (^{18}F-FDG PET) super scan involving the skeleton has been reported [4]. Increased skeletal-to-renal uptake ratios obtained with bone-seeking radiotracers have been associated with a variety of disorders [5]. In case of a super scan, skeletal uptake is very rapid and the percentage of injected Tc-99m MDP going to bone can be up to 85% [6]. Under this condition, a false-negative diagnosis may occur in clinical settings. Super scans have been described in relation to a variety of conditions such as metastatic disease, metabolic bone disease, and myeloproliferative disorders [1]. The imaging pattern of super bone scan in a variety of conditions is still different. For example, the characteristics of metastatic disease is diffuse heterogeneous radioactivity in the axial skeleton in the main, but diffuse homogeneous radioactivity in both the appendicular and axial skeletons in myeloproliferative disorders [1,7]. In metabolic disease, the super bone scan pattern is more uniform with peripheral skeletal distribution, including appendicular, skull and long bones.

The use of ^{18}F-FDG PET or computed tomography (CT) in the evaluation and management of patients with malignancy continues to increase. The radiopharmaceutical agent has the advantage of demonstrating all metastatic sites, and in the skeleton, it is taken to represent metabolism of tumor cells. In comparison with Tc-99m MDP bone scan, ^{18}F-FDG PET is more valuable for identifying bone-marrow-based disease as multiple myeloma [8]. In breast cancer, ^{18}F-FDG PET is highly sensitive mainly in diagnosis of early metastatic disease, which may still be confined to the bone marrow, as well as for the detection of lytic bone metastases [9]. ^{18}F-FDG PET also conveys the status of glucose metabolism in bone marrow when hematopoietic cytokine level changes [10].

We collected two patients with super bone scan, one with initial diagnosis of stage IV gastric cancer and the other with recurrent breast cancer. Both cases had ^{18}F-FDG PET/CT diagnosis simultaneously. The cytological results of bone marrow biopsy demonstrated evidence of malignant metastasis. We compared these two super bone scan patterns in detail and the imaging of Tc-99m MDP bone scan and ^{18}F-FDG PET/CT individually. The molecular mechanism of bone marrow metastasis resulting in the diffuse high bone turnover status of the super bone scan is proposed, based on a recent literature review.

Case presentations

Case 1

A 43-year-old man had suffered from low back pain for 3 months in 2007, before he came to our hospital. Tc-99m MDP bone scan and magnetic resonance imaging (MRI) were arranged for evaluation. The Tc-99m MDP bone scan revealed a super scan pattern with high skeletal-to-renal ratio (Fig. 1A). Pelvic MRI showed multiple marrow metastatic infiltrations. Bone marrow biopsy demonstrated metastatic carcinoma. Immunohistochemical staining revealed positive cytokeratin (CK)7 and faint CK20 characteristics, which had possible origins in the gastrointestinal system, such as the pancreas, liver, and stomach. Under clinic diagnosis of cancer of unknown primary site, ^{18}F-FDG PET/CT (GE, DST 16, USA) was arranged for further evaluation. The ^{18}F-FDG PET/CT imaging revealed a low-grade ^{18}F-FDG-avid tiny nodule (~1.1 cm) with a maximal standard uptake value (SUVmax) of 3 in the body portion of the stomach. Endoscopic biopsy showed grade III adenocarcinoma. No regional lymph nodal radioactivity was identified on ^{18}F-FDG PET/CT imaging. Based on whole body ^{18}F-FDG PET/CT imaging, functional bilateral kidneys were identified. Extensively disseminated, increased ^{18}F-FDG uptake in the axial skeleton was noted (Fig. 1B). Diffuse severe osteoporosis pattern was noted in the pelvis and sacrum on CT. High-grade ^{18}F-FDG avid hypodense metastatic tumor (SUVmax 9) in T12 was also noted (Fig. 1C). Thus, a poor prognosis, stage IV gastric cancer was diagnosed.

Case 2

A 57-year-old woman had been diagnosed with left breast, infiltrating ductal carcinoma, stage IIA (T2N0M0) in 1994. She received modified radical mastectomy, hormonal therapy and regional radiotherapy. Thereafter, she had regular follow-up in our clinic. There was no evidence of bone metastases on serial Tc-99m MDP bone scan before 2005. In May 2010, she experienced poor appetite and demonstrated severe body weight loss. High serum carcinoembryonic antigen level was noted as 80 ng/mL. Whole body ^{18}F-FDG PET/CT was indicated for suspicious recurrent breast cancer. On ^{18}F-FDG PET/CT imaging, bilateral functioning kidneys were identified. However, extensively increased marrow metabolism was noted in the axial skeleton (Fig. 2A), associated with mild osteoporosis pattern in the pelvic bones on CT. Under the impression of severe metastatic bone marrow disease, bone marrow biopsy was performed. The immunohistochemical stain

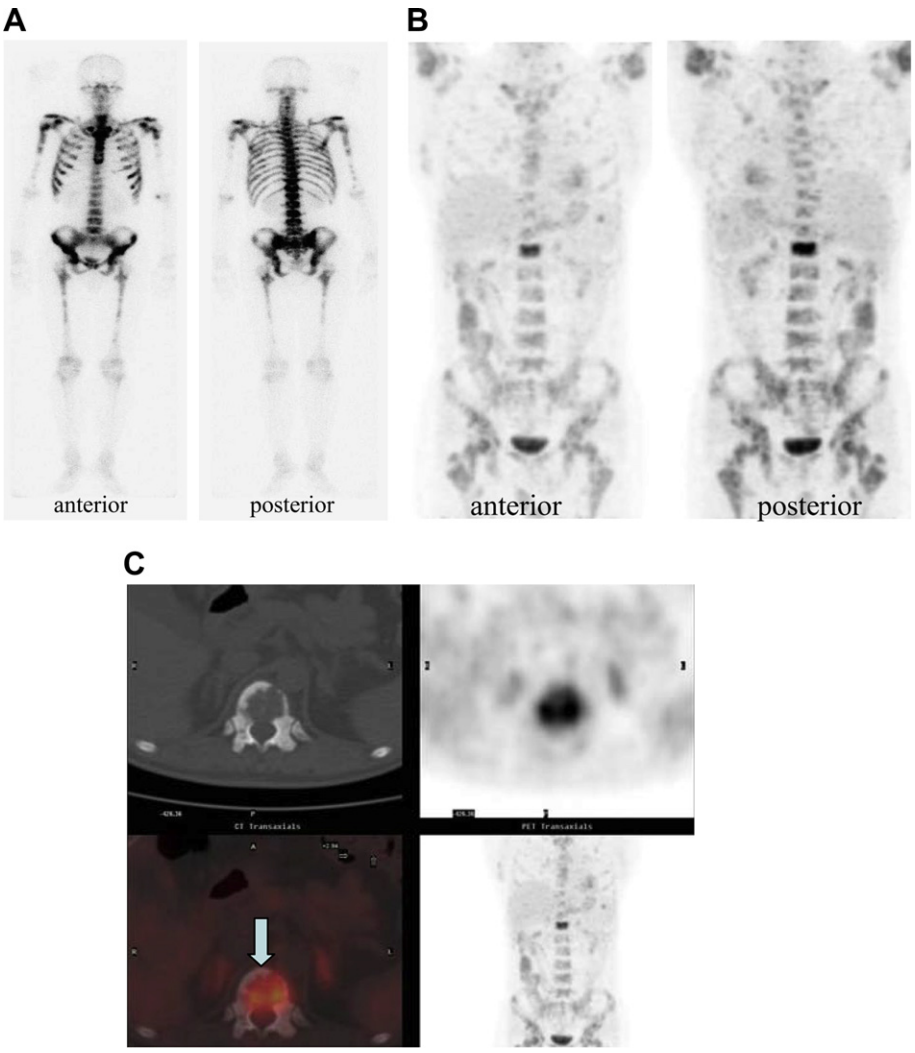

Figure 1. (A) In the patient diagnosed with gastric cancer, technetium-99m methyldiphosphonate bone scan revealed super bone scan pattern with absent renal radioactivity and diffusely mild heterogeneous skeletal radioactivity throughout the whole axial skeleton, ribs, head of clavicle, sternum, scapulae, proximal humeri and femora. (B) The 18F-FDG PET scan showed extensively incremental ^{18}F-FDG avid bone marrow metabolism with SUVmax 3 in the axial skeleton (significantly in ileum and sacrum) and proximal humeri and femora. (C) Focally high grade of ^{18}F-FDG avidity (SUVmax 9) was noted in T12. PET/computed tomography fusion imaging identified a space occupied by a consistently high grade of ^{18}F-FDG avid hypodense tumor associated with peripheral osteolysis (arrow). ^{18}F-FDG PET = 18-fluorodeoxyglucose positron emission tomography; SUVmax = maximal standard uptake value.

demonstrated neoplastic cells with positive CK, estrogen receptor and Her2/neu. The Tc-99m MDP bone scan consistently showed a super bone scan pattern (Fig. 2B). Significant left arm lymphedema was also noted. She received chemotherapy, targeted therapy, and bisphosphonate for advanced breast cancer. After 1 year of aggressive treatment, she underwent an ^{18}F-FDG PET/CT scan to evaluate treatment response, which revealed significantly reduced axial skeletal bone marrow activity (Fig. 2C). The follow-up Tc-99m MDP bone scan showed bilateral renal and soft tissue radioactivity, which was not consistent with typical imaging pattern of super bone scan (Fig. 2D). However, some progressive radioactivity in the left proximal femur was noted. The patient is still being followed up in our hospital.

Discussion

Cancer metastasis is the major cause of morbidity and death in cancer patients. The hypothesis of organ-specific metastasis is widely accepted. In 1889, Paget first proposed the "seed and soil" theory to describe metastasis. He considered the processes of metastasis did not occur by chance; rather, certain favored tumor cells with metastatic ability (the seed) had a specific affinity for the growth-enhancing milieu within specific organs (the soil, microenvironment) [11,12]. Bone marrow and bone are the environments with abundant blood flow and growth factors. Once the tumor successfully metastasizes to the bone marrow, it will trigger complicated interactions that are regulated by various growth factors among the tumor,

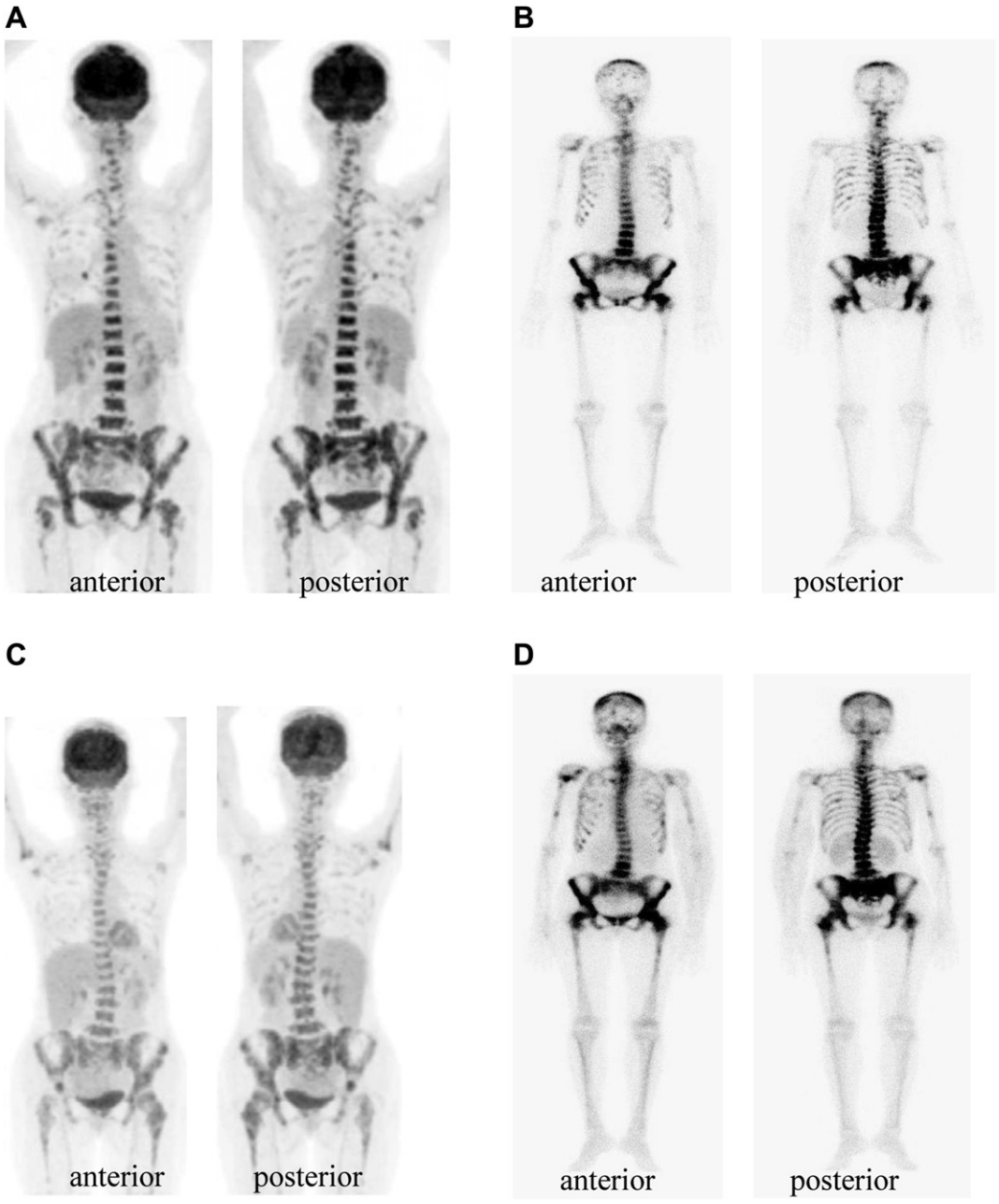

Figure 2. At initial diagnosis of recurrent breast cancer, ^{18}F-FDG PET/CT and Tc-99m MDP bone scan were performed. (A) ^{18}F-FDG PET/CT showed incrementally high grade of ^{18}F-FDG avid marrow metabolism (SUVmax 8) in the axial skeleton. (B) Tc-99m MDP bone scan revealed a typical super bone scan pattern. After aggressive cytotoxic treatment 1 year later, the follow-up images were shown as (C) ^{18}F-FDG PET/CT revealed treatment response, with significantly reduced axial skeletal bone marrow metabolism (SUVmax 4). (D) Tc-99m MDP bone scan revealed bilateral renal and soft tissue radioactivity, which was not consistent with typical imaging pattern of super bone scan. CT = computed tomography; ^{18}F-FDG PET = 18-fluorodeoxyglucose positron emission tomography; SUVmax = maximal standard uptake value; Tc-99m MDP = technetium-99m methyldiphosphonate.

osteoclasts and osteoblasts, resulting in different types of bone metastasis. It is clear that bone microenvironment is fertile for the growth of breast, prostate and lung cancer. Bone metastasis occurs in 70% of patients with advanced breast and prostate cancer, in terms of osteotropic tumor [13]. In cancers of the thyroid, lung and kidneys bone metastasis occurs in 30—40% of patients, but in cancers from the gastrointestinal tract, bone metastasis is found in <10% of cases. In metastasis-related super bone scan, prostate cancer is the most common cause, with up to 17% [14]. In women, breast cancer is the most common cause [15]. In this study, we collected one case of gastric cancer with initial diagnosis of stage IV bone metastasis, and one case of breast cancer with recurrence after 20 years. Both cases had a super bone scan pattern, which is rare for such cases in the literature.

Characteristics of the metastatic super bone scan imaging patterns of both cases were diffuse heterogeneous

high MDP radioactivity, mainly in the axial skeleton (Figs. 1A and 2B). However, the distribution varied. We know that in imaging of gastric cancer patients, higher MDP avid radioactivity is distributed through flat bones such as the iliac crest, sternum and proximal end femur, which have red marrow distribution [12,13]. By contrast, our case of breast cancer showed higher MDP avid radioactivity in the lumbar spine. Furthermore, regional photopenia was noted in the left upper ribs, probably related to prior radiotherapy. Both cases had positive bone marrow biopsies, which represent a heterogeneous massive tumor burden in the bone cavity, associated with diffuse high bone turnover [16,17]. According to the above findings, it was still uncertain whether the threshold of tumor burden or a chemical entity was related to the condition of the super bone scan. In comparison with ^{18}F-FDG PET/CT imaging, incremental ^{18}F-FDG avidity (SUVmax 8—9) was consistent with the super bone scan pattern in the breast cancer patient (Fig. 2A and B). However, there was some discrepant distribution between ^{18}F-FDG PET/CT and bone scan in the gastric cancer case (Fig. 1A and B). There was a focal high ^{18}F-FDG uptake in T12 (SUVmax 9) (Fig. 1C). This phenomenon represents diffuse high bone turnover, where super bone scan is not only consistent with diffuse tumor burden, but also certain neoplasm-related endocrine factors, such as parathyroid hormone-related peptide (PTHrP) [13]. In an osteolytic metastasis model of breast cancer [18,19], breast cancer cells secrete PTHrP binding the parathyroid hormone 1 receptor that induces formation of osteoclasts. In turn, bone resorption by osteoclasts releasing growth factors from bone matrix that stimulate tumor growth and bone destruction. Both present cases contained abundant tumor burden as shown on ^{18}F-FDG PET/CT imaging and showed a super bone scan pattern. Interestingly, in the case of breast cancer, the phenomenon of super bone scan was reversible after aggressive treatment (Fig. 2B and D), which is an uncommon result. To the best of our knowledge, this has not often been mentioned before. Reversible super bone scan after cytotoxic therapy still demonstrates the relationship between osteotrophic metastatic neoplasm cells and bone marrow/bone microenvironment [13,18,19]. It would be an interesting and valuable area of research to establish large-scale clinical correlation based on different cancer entities in the future.

Molecular medicine provides new clues to explain the regulation of the microenvironment in bone marrow/bone-related to stem cells [20,21]. Super bone scan represent a diffuse high bone turnover rate, as noted in 1975, and it is due to diffuse infiltrating marrow metastasis. Based on the seed-and-soil theory, the initiation of super bone scan is not only the result of massive osteotrophic metastatic cancer infiltrating the bone marrow/bone microenvironment, but also triggering of serial endocrine systems.

In conclusion, according to integration of both imaging findings and results of bone marrow biopsy, the authors consider that disseminated malignant spread in bone marrow and also neoplasm-related endocrine factors support the phenomenon of a super bone scan.

References

[1] Buckley O, O'Keeffe S, Geoghegan T, Lyburn ID, Munk PL, Worsley D, et al. 99mTc bone scintigraphy superscans: a review. Nucl Med Commun 2007;28:521—7.

[2] Frankel RS, Johnson KW, Mabry JJ, Johnston GS. "Normal" bone radionuclide imaging with diffuse skeletal lymphoma. A case report. Radiology 1974;111:365—6.

[3] Osmond III JD, Pendergrass HP, Potsaid MS. Accuracy of 99mTc-diphosphonate bone scans and roentgenograms in the detection of prostate, breast and lung carcinoma metastases. Am J Roentgenol 1975;125:972—7.

[4] Su HY, Liu RS, Liao SQ, Wang SJ. F-18 FDG PET superscan. Clin Nucl Med 2006;31:28—9.

[5] Cheng TH, Holman BL. Increased skeletal: renal uptake ratio: etiology and characteristics. Radiology 1980;136:455—9.

[6] Constable AR, Cranage RW. Recognition of the superscan in prostatic bone scintigraphy. Br J Radiol 1981;54:122—5.

[7] Han R, Nikpoor N. Different scintigraphic patterns of superscan. Am J Roentgenol 2006;186:A145—8.

[8] Fogelman I, Cook G, Israel O, Van der Wall H. Positron emission tomography and bone metastases. Semin Nucl Med 2005; 35:135—42.

[9] Ben-Haim S, Israel O. Breast cancer: role of SPECT and PET in imaging bone metastases. Semin Nucl Med 2009;39:408—15.

[10] Yao WJ, Hoh CK, Hawkins RA, Glaspy JA, Weil JA, Lee SJ, et al. Quantitative PET imaging of bone marrow glucose metabolic response to hematopoietic cytokines. J Nucl Med 1995;36: 794—9.

[11] Ribatti D, Mangialardi G, Vacca A. Stephen Paget and the 'seed and soil' theory of metastatic dissemination. Clin Exp Med 2006;6:145—9.

[12] Paget S. The distribution of secondary growths in cancer of the breast. Lancet 1889;133:571—3.

[13] Buijs JT, van der Pluijm G. Osteotropic cancers: from primary tumor to bone. Cancer Lett 2009;273:177—93.

[14] Manier SM, Van Nostrand D. Super bone scan. Semin Nucl Med 1984;14:46—7.

[15] Benítez A, Torres M, García A, Rebollo AC, Pacheco C, Vallejo JA, et al. Radionuclide bone scanning in patients with breast carcinoma. Rev Esp Med Nucl 1998;17:435—41.

[16] Kanazawa K, Isozaki E. "Super bone scan" in a case of diffuse bone marrow metastasis of gastric adenocarcinoma. Intern Med 2009;48:1719—20.

[17] Ahn JB, Ha TK, Kwon SJ. Bone metastasis in gastric cancer patients. J Gastric Cancer 2011;11:38—45.

[18] Roodman GD. Mechanisms of bone metastasis. N Engl J Med 2004;350:1655—64.

[19] Mundy GR. Mechanisms of bone metastasis. Cancer 1997; 80(Suppl):1546—56.

[20] Bianco P. Minireview: the stem cell next door: skeletal and hematopoietic stem cell "niches" in bone. Endocrinology 2011;152:2957—62.

[21] Bianco P. Bone and the hematopoietic niche: a tale of two stem cells. Blood 2011;117:5281—8.